Applied Energy 299 (2021) 117283

Contents lists available at ScienceDirect

Applied Energy

journal homepage: www.elsevier.com/locate/apenergy

A novel multi-objective method with online Pareto pruning for multi-year optimization of rural microgrids

Marina Petrelli [a,*], Davide Fioriti [b], Alberto Berizzi [a], Cristian Bovo [c], Davide Poli [b]

[a] Politecnico di Milano, Energy Department, Via Giuseppe La Masa 34, Milano, Italy
[b] Università di Pisa, Department of Energy, Systems, Territory and Construction Engineering, Via Carlo Francesco Gabba 22, Pisa, Italy
[c] Università di Pavia, Facoltà di Ingegneria, Via Adolfo Ferrata 5, Pavia, Italy

ARTICLE INFO

Keywords:
Hybrid minigrid sizing
Mixed-Integer Linear Programming (MILP)
eps-constraint method
Online pareto filter
Holistic design
Off-grid PV-wind-battery-diesel system

ABSTRACT

Decentralized hybrid energy systems are promising long-lasting solutions to support socio-economic development in compliance with environmental concerns. Traditionally, microgrid planning has mainly focused on economics only, sometimes with reliability or environmental considerations, and the project costs have been estimated by approximating the multi-year operation of the system with a single-year approach, thus neglecting long-term phenomena. We propose a multi-objective multi-year method to plan microgrids in the Global South, accounting for socio-economic (Net Present Cost, job creation), security (public lighting coverage) and environmental impacts (carbon emissions, land use); the entire multi-year lifespan of the project is considered, including demand growth and assets degradation. The advanced version of the augmented ε-constraint algorithm, denoted as A-AUGMECON2, is here proposed to efficiently solve the multi-objective model, by using a novel pruning algorithm that avoids solving redundant optimizations. The method is applied to an isolated community in Uganda. The approach successfully quantifies the trade-off between local long-term impacts, supporting policy makers and local developers in designing effective policies and actions. In particular, our results suggest that the environmental targets can be aligned with the project economics, and that the financial impact of public lighting is limited, which encourages its implementation in electrification projects. Conversely, optimal land use and job creation lead to high economic and environmental costs, highlighting the need for a trade-off for policy and business decision makers. Moreover, the novel A-AUGMECON2 algorithm enables reducing by 48% the computational requirements of the standard AUGMECON2, extending the application of multi-objective methodologies to more complex problems.

1. Introduction

1.1. Motivation

As stated in the Sustainable Development Goals, achieving universal electricity access is a key priority of the international community [1]. Electricity is a well-known determinant for social development [2], as it enables the use of modern appliances, replaces lower quality energy sources, such as kerosene, wood, and charcoal, stimulates economic growth, and improves well-being [3,4]. However, currently, almost 800 million people live without access to electricity, and most of them are located in rural areas in Sub-Saharan Africa [5], which are often difficult to reach. Additionally, these remote areas typically rely on subsistence economy, with very basic electricity needs, such as lighting and charging of mobile phones; therefore, depending on the location, extending the public power grid may be considered too expensive and not-worth in the short-term. Conversely, decentralized solutions such as microgrids can be promising and cost-effective solutions, but adequate optimization tools shall be developed to account for the multi-faceted context of rural areas in the Global South for the entire lifetime of the project.

Multi-objective optimization has proven to enable evaluating the trade-offs between different decision criteria in the energy sector, in particular for rural electrification projects, where different types of stakeholders with different priorities may be involved (companies, public institutions, NGOs) and a thorough analysis of the relationships between the economic, environmental and social impacts on the community is required [6]. The corresponding output, typically being a Pareto frontier, provides the decision maker with a more comprehensive view of the outcomes of their choices so that more informed decisions can be taken, also based on cultural and site-specific characteristics which could hardly be described within the algorithm.

* Corresponding author.
E-mail address: marina.petrelli@polimi.it (M. Petrelli).

https://doi.org/10.1016/j.apenergy.2021.117283
Received 23 February 2021; Received in revised form 8 June 2021; Accepted 10 June 2021
Available online 23 June 2021

Moreover, when dealing with rural areas, scarcity of information is often an issue hindering the effective calibration of a single-objective optimization, which entails the identification of weights or bounds, heavily influencing the final solution [7,8].

Hence, it is timely and useful to develop a multi-objective planning methodology able to address economic, social, and environmental objectives, besides accounting for the multi-year characteristics of the project and including the degradation model of the assets. On the other side, in order to tackle the increased complexity in planning methodologies, it is also important to develop novel techniques to more efficiently address multi-objective optimization.

1.2. Literature analysis

Standard microgrid sizing tools usually focus on single-year economics-only optimizations in order to reduce the complexity of the analysis. In [9–11], the least-cost solution is identified by optimizing the generating portfolio together with the scheduling strategy of the first year, assumed to be representative of all the subsequent years. Likewise, the operating costs will also recur from year to year. Therefore, cost is considered as the only determining factor in the effectiveness of the rural electrification process. These assumptions hardly match the complex circumstances of off-grid microgrids in the Global South, given the multiplicity of impacts on the community involved, the intrinsic long-lasting nature of the system, the significant load growth and the assets degradation over the years. Neglecting these aspects in favour of more details on short-term features can lead to sub-optimal designs, since long-term dynamics are more relevant in rural contexts and significantly affect the optimal choice of the system [12].

Only few studies have recently adopted a multi-year approach, partially integrating the multi-year characteristics of the system [13–15]; namely, load growth [13,15] and storage capacity reduction, regardless of how the batteries are used [14,15]. Actually, the pace at which batteries degrade is strongly linked to their operation [16] and this has significant impact on the optimal microgrid planning and scheduling [17]. Moreover, renewable energy generators are subject to performance deteriorations too [18,19], and this influences their optimal size.

A growing interest in environmental protection issues has led various scholars to also include an assessment of carbon emissions in their analyses, as a limit not to be exceeded [20], or as monetary cost to be minimized [15,21], or as additional objective function [22–25]; however, Life-cycle Assessment (LCA), which quantifies the emissions along the whole life-cycle of an asset, is rarely adopted [20,24], and generally only direct emissions are taken into account [15,21–23,25], resulting in incomplete and sometimes misleading evaluations.

In addition to this, the importance of considering the social impact of rural electrification projects is increasingly recognized and demanded as an indispensable element of system planning tools [6]. Nonetheless, very few multi-objective algorithms have been developed including social assessments, mostly through the evaluation of employment generation [26–28].

A popular and consolidated approach for holistic analysis of rural electrification projects is to use Multi-Criteria Decision Analysis (MCDA) [29–32], which is more prone to including social and qualitative decision criteria. However, MCDA cannot determine the generation mix and the scheduling strategy and is not able to efficiently manage different configurations of hybrid systems. Hence, these aspects must be analysed separately and MCDA is used for ex-ante [31] or ex-post [32] assessments, but planning tools are still needed.

Therefore, it turns out that the literature lacks a holistic multi-objective optimization that addresses all the aforementioned shortcomings.

In the scope of Mixed-Integer Linear Programming (MILP) optimization, which is the formulation adopted in this study, the most common approaches to solve multi-objective problems are the weighted sum method [33,34] and the ε-constraint method [35–37]. The latter has the advantage of being able to represent the entire Pareto frontier independently of its shape; moreover, its results are not influenced by normalization issues and it generally has better computational performances [7,8]. In particular, the augmented ε-constraint method (AUGMECON2) has been developed as an advancement of the traditional ε-constraint method [38,39] and, currently, it is a well consolidated method, widely adopted to solve a diverse portfolio of problems in the energy sector [36,37,40,41].

However, AUGMECON2 presents two interrelated drawbacks: (1) when complex algorithms with more than two objective functions are optimized, the computational burden may become extremely large because of the presence of redundant iterations; (2) the higher the desired resolution of the Pareto frontier, the more the redundant points. The former issue needs an advancement of the methodology, while the latter, which is related to the readability of the results and the choice of the final point, could be faced by one of the post-Pareto selection methods available. These can be grouped into three major categories: offline pruning algorithms to reduce the number of Pareto points [42,43]; clustering algorithms to identify and group similar solutions [44]; mathematical methods to select a single final point [45,46]. This additional step requires further computational resources, thus exacerbating the first issue.

Most of the recent literature still considers AUGMECON2 as the most up-to-date development of the ε-constraint method, as proven by its recent use in a wide variety of scientific literature also beyond the energy sector [47,48]. The very first efforts in advancing the methodology have been proposed in [49], partially addressing the issue of redundant optimizations. Nonetheless, the scope of [49] is limited to a theoretical approach applied on a test knapsack problem to highlight the efficiency of the algorithm, yet the performances of AUGMECON2 could be further improved. For these reasons, AUGMECON2 is selected by the authors to solve the multi-objective multi-year optimization under study, and its two main shortcomings are faced by a novel methodology, aimed at providing better computational performances and improved readability of the Pareto frontier by means of an online filter of redundant optimizations.

1.3. Contributions

To the best of the authors' knowledge, the proposed modified version of AUGMECON2, here denoted as A-AUGMECON2, goes beyond the state of the art both in terms of advancements of the mathematical properties of the algorithm, fully addressing the issue of redundant simulations, and in terms of practical application of such novel approach, being it its first application to energy systems. Moreover, this is the first study providing such a comprehensive evaluation of rural microgrid projects, discussing both the multi-objective and multi-year features of the problem. In short, the main novelties are discussed below.

1. Development of a multi-objective multi-year planning methodology able to efficiently optimize and simulate the operation of the entire lifetime of a project, using economic (Net Present Cost), social (Job Creation and Public Lighting), and environmental (Life-cycle emissions and Land use) objective functions.
2. Detailed modelling of the degradation of the assets of the microgrid performed by a custom iterative approach decomposing the full non-linear model into the consecutive optimization of a MILP problem.
3. Development of the A-AUGMECON2 methodology that reduces the computational requirements of the standard AUGMECON2, using a novel pruning algorithm that avoids the simulation of redundant iterations and enables the introduction of the first two novelties while keeping a good tractability of the algorithm.

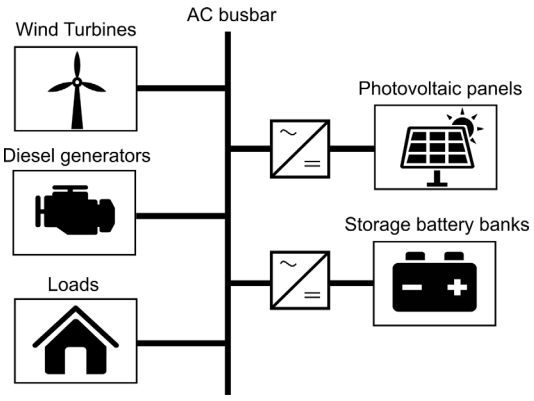

Fig. 1. Microgrid layout [17].

2. Microgrid planning

In this section, the model for the multi-year planning of off-grid microgrids is described. The formulation, based on [17], accounts for detailed simulations of the entire lifetime of the project, including the operational effects of the generation and storage degradation and of battery variable efficiency.

2.1. Description

The configuration of the microgrid considered in this study and shown in Fig. 1 is aimed at representing the typical off-grid system in the Global South: it includes photovoltaic panels of type p, wind turbines of type w, fuel-fired generators of type g, and battery storage of type b, coupled at the AC busbar to supply the demand. The proposed model adopts a single-node equivalent, which represents an effective and well-established characterization of this kind of system [11,25], where generation assets are usually centralized and the distribution network is typically radial.

The list of all the quantities used in the following subsections to model the planning and operation phase of the microgrid is presented in Table 1.

2.2. The objective functions

2.2.1. Net present cost

As for microgrid investments, the Net Present Cost is typically considered as economic objective function, to be minimized, according to Eqs. (2)–(8). Its formulation takes into account the investment costs IC_i, the operation and maintenance charges $O\&M_i$, the replacement costs RC_i of batteries and diesel generators (the other components have service life longer than project duration), and the residual values RV_i of the assets at the end of the project lifetime. Given the cumulative modelling of DG replacement charges as in (5), there is no need to consider DG residual value.

$$\min NPC = \sum_i (IC_i + O\&M_i + RC_i - RV_i) \tag{1}$$

$$IC_i = N_i \cdot c_i \tag{2}$$

$$O\&M_{i\setminus\{g\}} = N_i \cdot m_i \sum_y d_y \tag{3}$$

$$O\&M_g = \sum_{y,h} d_y (m_g \cdot U_{y,h,g} + \pi^f \cdot FC_{y,h,g}) \tag{4}$$

$$RC_g = \frac{c_g}{h_g^{life}} \sum_{y,h} d_y \cdot U_{y,h,g} \tag{5}$$

$$RC_b = N_b \cdot c_b \sum_{y,h} d_y (k_{y,h,b} - k_{y,h-1,b}) \tag{6}$$

$$RV_{i\setminus\{g,b\}} = d_{|Y|} \cdot N_i \cdot c_i \cdot \frac{y_i^{life} - |Y|}{y_i^{life}} \tag{7}$$

$$RV_b = d_{|Y|} \cdot c_b \frac{C^{res}_{|Y|,|H|,b} - N_b \underline{C}_b}{\overline{C}_b - \underline{C}_b} \tag{8}$$

2.2.2. Emissions

Environmental objectives have been increasingly included in energy projects planning, due to climate-change concerns. To perform an accurate evaluation of the microgrid global impact, emissions have been considered in the proposed methodology in terms of LCA, i.e. accounting for construction, installation, operation and disposal of the assets. The minimization of total emission allows to evaluate solutions in line with the increasing pressure of governments for high shares of renewables. The mathematical formulation of CO_2 emissions is reported in (9)–(13). Fuel-fired generators are the only contributing emissions during the operation phase ($OCO2_g$).

$$\min CO2 = \sum_i CCO2_i + OCO2_i \tag{9}$$

$$CCO2_{i\setminus\{g,b\}} = N_i \cdot e_i \tag{10}$$

$$CCO2_b = \left[1 + \sum_{y,h} (k_{y,h,b} - k_{y,h-1,b})\right] N_b \cdot e_b \tag{11}$$

$$CCO2_g = N_g \cdot e_g + \sum_{y,h} \frac{U_{y,h,g}}{h_g^{life}} \cdot e_g \tag{12}$$

$$OCO2_g = FC_{y,h,g} \cdot e_g^{op} \tag{13}$$

2.2.3. Land use

The local environmental impact of the microgrid is taken into account by including in the analysis the minimization of the space required for the installation of the different assets [26]. The importance of this variable for decision makers is strictly related to the specific conditions of the area where the system needs to be installed; for example, land occupation may become a sensitive issue when the community is based in a protected area. The land use (LU) minimization is therefore considered in (14).

$$\min LU = \sum_i N_i \cdot lo_i \tag{14}$$

2.2.4. Jobs creation

Energy planning can promote local jobs, as a consequence of the assets installation and operation, which are incorporated in the proposed multi-objective method by means of a maximization problem [26–28]. The mathematical formulation of the job creation JC, detailed in (15)–(18), is a function of the jobs generated throughout the value chain of each asset (CJC_i). Moreover, the contribution related to fuel consumption for fuel-fired generators is accounted by means of a separate variable (OJC_g).

$$\max JC = \sum_i CJC_i + OJC_g \tag{15}$$

$$CJC_{i\setminus\{g\}} = N_i \cdot j_i \tag{16}$$

$$CJC_g = N_g \cdot j_g + \sum_{y,h} U_{y,h}^{dg} \cdot \frac{j_g}{y_g^{life}} \tag{17}$$

$$OJC_g = \sum_{y,h} P_{y,h,g}^{dg} \cdot j_g^f \tag{18}$$

2.2.5. Public lighting coverage

Finally, public lighting (PL) is considered and included in the optimization, as it is an important enabler of better living conditions, including but not limited to improved security, recreational and educational activities. For this reason, street lights are considered as priority loads and they are not subject to curtailments: once a street light is installed, it must be supplied during the dark hours. The total need of

Table 1
Definition of indexes, parameters and variables for microgrid planning.

Indexes			
h	Hours	y	Years
g	Diesel generators (DG)	p	Photovoltaic panels (PV)
w	Wind turbines (WT)	b	Batteries (BESS)
i	Components, $i \in \{g, p, w, b\}$		
Parameters			
M	Big constant	$\|H\|$	Number of hours per year
$\|Y\|$	Project lifetime	y_i^{life}	Component lifetime
c_i	Unit capital cost	m_i	Unit maintenance cost
e_i	Unit installation emissions	e_i^{op}	Unit operation emissions
lo_i	Unit land occupation	j_i	Unit jobs from value chain
j_g^f	Unit jobs form fuel use	$L_{y,h}^{tot}$	Total lighting demand
d_y	Discount factor	f^u	Max unmet demand fraction
δ	Demand growth rate	γ_z	Forecast error of z
$P_{y,h,p}^{pv}$	Available PV power	$P_{y,h,w}^{wt}$	Available WT power
$\rho_{y,h,p}^{pv}$	Linear PV degradation rate	$\rho_{y,h,p}^{wt}$	Linear WT degradation rate
π^f	Cost of fuel	h_g^{life}	Total DG working hours
$\overline{P}_g$	Max DG power	$\underline{P}_g$	Min DG power
a, b	Fuel consumption coefficients	DOD_b	Depth of Discharge
$\eta_{y,h,b}$	Power-dependent efficiency	$\overline{\eta}_b$	Max BESS efficiency
$\overline{C}_b$	Max BESS capacity	$\underline{C}_b$	Min (aged) BESS capacity
$C_{y,h,b}^{res}$	Total residual BESS capacity	$k_{y,h,b}$	BESS replacement counter
$\overline{PQ}_b$	Max power-to-energy ratio	$PQ_{y,h,b}$	Power-to-energy ratio
$Q_{y,h,b}^{thr}$	Cumulative throughput	$n_{y,h,b}^{cyc}$	Working max number of cycles
Variables			
NPC	Net present cost	IC_i	Initial investment cost
$O\&M_i$	O&M cost	RC_i	Replacement cost
RV_i	Residual value	$CO2$	Total LCA emissions
$CCO2_i$	Emissions from installation	$OCO2_i$	Emissions from O&M
LU	Total land use	JC	Total job creation
CJC_i	Jobs from whole value chain	OJC_g	Jobs from fuel use
PL	Public lighting coverage (%)	N_i	Number of units installed
$D_{y,h}$	Load demand	$D_{y,h}^u$	Unmet demand
$L_{y,h}$	Fulfilled lighting demand	$P_{y,h}^{ren}$	Renewable power injected
$R_{y,h}$	Total reserve requirement	$FC_{y,h,g}$	Fuel consumption
$P_{y,h,g}^{dg}$	Power produced by DG	$R_{y,h,g}^{dg}$	Reserve provided by DG
$U_{y,h,g}$	Active DG units (integer)	$w_{y,h,b}^{dch}$	Binary variable on BESS state
$P_{y,h,b}^{dch}$	Discharging power of BESS	$P_{y,h,b}^{ch}$	Charging power of BESS
$R_{y,h,b}^{sb}$	Reserve provided by BESS	$Q_{y,h,b}$	Energy level of BESS

street lights to cover the whole area and the related power profile $L_{y,h}^{tot}$ are assessed. Eq. (19) maximizes the coverage of the service, expressed as the share (%) of the total requirement which is actually fulfilled.

$$\max PL = \frac{L_{y,h}}{L_{y,h}^{tot}} \cdot 100 \tag{19}$$

2.3. Main constraints

The electric balance is guaranteed by (20), while (21) describes the linear growth of the demand. A reasonable amount of load shedding, to be defined according to local socio-economic information, is generally admitted in rural areas, as long as it enables a reduction of the electricity tariff. Hence, Eqs. (22)–(23) rule the fraction of unmet demand. The dispatched power from renewable sources is limited in (24) by their availability and by the degradation of the components over time.

$$\sum_b \left(P_{y,h,b}^{dch} \cdot \eta_{y,h,b} - \frac{P_{y,h,b}^{ch}}{\eta_{y,h,b}} \right) + P_{y,h}^{ren} + \\ + \sum_g P_{y,h,g}^{dg} + D_{y,h}^u = D_{y,h} + L_{y,h} \tag{20}$$

$$D_{y,h} = D_{1,h}(1+\delta)^y \tag{21}$$

$$D_{y,h}^u \le D_{y,h} \tag{22}$$

$$\sum_h D_{y,h}^u \le f^u \sum_h D_{y,h} \tag{23}$$

$$P_{y,h}^{ren} \le \sum_p N_p \cdot P_{y,h,p}^{pv} \cdot \rho_{y,h,p}^{pv} + \sum_w N_w \cdot P_{y,h,w}^{wt} \cdot \rho_{y,h,w}^{wt} \tag{24}$$

Constraints (25)–(28) detail the mathematical description of the fuel-fired generators for every technology g taken into consideration, and ensure their correct operation and their support to reserve requirements.

$$FC_{y,h,g} = a \cdot U_{y,h,g} + b \cdot P_{y,h,g}^{dg} \tag{25}$$

$$P_{y,h,g}^{dg} + R_{y,h,g}^{dg} \le \overline{P}_g \cdot U_{y,h,g} \tag{26}$$

$$P_{y,h,g}^{dg} \ge \underline{P}_g \cdot U_{y,h,g} \tag{27}$$

$$U_{y,h,g} \le N_g \tag{28}$$

The equation block from (29) to (35) describes the model of the battery storage by technology b. While (29) depicts the energy balance in the battery, (30) and (31) detail the maximum and the minimum state of charge of the battery. It is worth noticing that $C_{y,h,b}^{res}$ models the total capacity of the battery, accounting for its degradation as stated in the following subsection. The power limits of the batteries are instead managed by constraints (32)–(35).

$$Q_{y,h,b} = Q_{y,h-1,b} + (P_{y,h,b}^{ch} - P_{y,h,b}^{dch})\Delta h \tag{29}$$

$$Q_{y,h,b} \le C_{y,h,b}^{res} \tag{30}$$

$$Q_{y,h,b} \ge N_b \cdot \overline{C}_b(1 - DOD_b) + R_{y,h,b}^{sb} \cdot \Delta h \tag{31}$$

$$P_{y,h,b}^{dch} + R_{y,h,b}^{sb} \le C_{y,h,b}^{res} \cdot \overline{PQ}_b \tag{32}$$

$$P_{y,h,b}^{ch} \le C_{y,h,b}^{res} \cdot \overline{PQ}_b \tag{33}$$

$$P_{y,h,b}^{dch} \le w_{y,h,b}^{dch} \cdot M \tag{34}$$

$$P_{y,h,b}^{ch} \le (1 - w_{y,h,b}^{dch}) \cdot M \tag{35}$$

Finally, the reserve requirements to cover short-term variations of demand and renewable generation are detailed in (36). These shall be

covered by the reserve bands of the batteries and fuel-fired generators, modelled in (37).

$$R_{y,h} = \gamma_d \cdot D_{y,h} + \gamma_{pv} \sum_p N_p \cdot p^{pv}_{y,h,p} + \gamma_{wt} \sum_w N_w \cdot p^{wt}_{y,h,w} \tag{36}$$

$$R_{y,h} \leq \sum_g R^{dg}_{y,h,g} + \sum_b R^{sb}_{y,h,b} \cdot \eta_{y,h,b} \tag{37}$$

2.4. The model of the battery efficiency

The efficiency $\hat{\eta}_{y,h,b}$ of the battery system is calculated as function of the power-to-energy ratio [16,17]: the higher the power flow from the battery, the lower the efficiency. In particular, a step-wise function ($\eta_b(PQ_{y,h,b})$) dependent upon the power ratio $PQ_{y,h,b}$, computed as in (38), is used to model the efficiency in every time step, as detailed in (39).

$$PQ_{y,h,b} = \frac{P^{ch}_{y,h,b} + P^{dch}_{y,h,b}}{N_b \cdot \overline{C}_b} \tag{38}$$

$$\hat{\eta}_{y,h,b} = \eta_b(PQ_{y,h,b}) \tag{39}$$

It is worth noticing that the direct implementation of the efficiency model of $\hat{\eta}_{y,h,b}$ in the previous section, i.e. setting $\hat{\eta}_{y,h,b} = \eta_{y,h,b}$, would make the problem significantly non-linear and hard to solve. For this reason, the iterative approach described in Section 2.6 is used.

2.5. The degradation of the battery system

The storage system is critical for most off-grid applications and its degradation can affect the profitability of the system, thus the battery model accounts for the degradation as in [17]. In particular, the residual capacity $\hat{C}^{res}_{y,h,b}$ of the battery defined in (41) is calculated as a function of the energy throughput $Q^{thr}_{y,h,b}$, detailed in (40). The formulation accounts for the variable degradation rate depending on charging and discharging power-to-energy ratio, modelled by the coefficient on maximum number of cycles $n^{cyc}_{y,h,b}(PQ_{y,h,b})$. When the useful battery capacity falls below a given threshold ($\underline{C}_b$), the battery is replaced, the available capacity is restored to the initial value and the counter $k_{y,h,b}$ stating the number of replacements is updated.

$$Q^{thr}_{y,h,b} = Q^{thr}_{y,h-1,b} + (P^{ch}_{y,h,b} + P^{dch}_{y,h,b})\Delta h \tag{40}$$

$$\hat{C}^{res}_{y,h,b} = \begin{cases} \hat{C}^{res}_{y,h-1,b} - \dfrac{\left(1 - \underline{C}_b/\overline{C}_b\right)\left(Q^{thr}_{y,h,b} - Q^{thr}_{y,h-1,b}\right)}{2n^{cyc}_{y,h,b}(PQ_{y,h,b})DOD_b} & \hat{C}^{res}_{y,h-1,b} \geq N_b\underline{C}_b \\ N_b\overline{C}_b & \hat{C}^{res}_{y,h-1,b} < N_b\underline{C}_b \end{cases} \tag{41}$$

Similarly to the variable efficiency model, setting $\hat{C}^{res}_{y,h,b} = C^{res}_{y,h,b}$ would mean to include in the main model a non-linear battery degradation model. In the following subsection a simplified iterative approach is proposed to overcome this complexity.

2.6. The iterative model

The model discussed in Sections 2.4 and 2.5 is significantly non-linear. Therefore, based on the iterative approach discussed in [17], the non-linearities of variables $C^{res}_{y,h,b}$ and $\eta_{y,h,b}$ are calculated externally to the MILP with off-line computations, as depicted in Fig. 2. To do so, the two variables are modelled as in (42) and (43), where parameters $\alpha_{y,h,b}\big|_{it}$ and $\beta_{y,h,b}\big|_{it}$ vary in the range 1÷100% and represent the hourly available storage capacity and efficiency with respect to their nominal values $N_b\overline{C}_b$ and $\overline{\eta}_b$. $\alpha_{y,h,b}\big|_{it}$ and $\beta_{y,h,b}\big|_{it}$ are updated in every iteration it to account for such non-linear phenomena in a MILP model, using a computationally efficient procedure.

$$C^{res}_{y,h,b} = \alpha_{y,h,b}\big|_{it} \cdot N_b \cdot \overline{C}_b \tag{42}$$

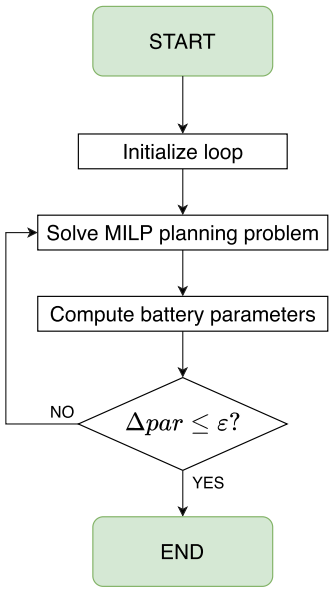

Fig. 2. Iterative procedure coping with non-linearities [17].

$$\eta_{y,h,b} = \beta_{y,h,b}\big|_{it} \cdot \overline{\eta}_b \tag{43}$$

As shown in Fig. 2, after each MILP iteration, the values of $\alpha_{y,h,b}\big|_{it+1}$ and $\beta_{y,h,b}\big|_{it+1}$ for the following iteration ($it+1$) are computed as in (44) and (45), based on the values of $\hat{C}^{res}_{y,h,b}$ and $\hat{\eta}_{y,h,b}$ calculated downstream of the planning procedure of the current iteration it. The algorithm stops when the relative changes of the parameters over consecutive simulations fall below a given threshold; more details on the procedure are discussed in [17].

$$\alpha_{y,h,b}\big|_{it+1} = \frac{\hat{C}^{res}_{y,h,b}\big|_{it}}{N_b \cdot \overline{C}_b} \tag{44}$$

$$\beta_{y,h,b}\big|_{it+1} = \frac{\hat{\eta}_{y,h,b}\big|_{it}}{\overline{\eta}_b} \tag{45}$$

The effectiveness of the approach has been validated in [17], by comparing the iterative procedure with the full MILP formulation and showing that the proposed method provides a very good approximation of the optimal solution, while being extremely more efficient.

3. Multi-objective optimization

A generic multi-objective optimization can be expressed as follows:

$$\begin{aligned} &\max f(\mathbf{x}) = [f_1(\mathbf{x}), f_2(\mathbf{x}), \dots, f_p(\mathbf{x})]^T \\ &s.t. y_i(\mathbf{x}) \leq 0 \qquad i \in 1...m \\ &\quad h_l(\mathbf{x}) = 0 \qquad l \in 1...q \\ &\quad \mathbf{x} = [x_1, x_2, \dots, x_n]^T \end{aligned} \tag{46}$$

where $f(\mathbf{x})$ is the p-dimensional vector of objective functions, defined by the n-dimensional vector of decision variables $\mathbf{x}$. The problem is subject to m inequality constraints and q equality constraints. For the sake of simplicity, we describe a problem where all objective functions are maximized, but the same considerations follow also for minimization or mixed maximization/minimization problems.

The goal of multi-objective optimizations is to find the solutions as close as possible to the Pareto frontier, which is composed by the set of so-called non-dominated points, i.e. solutions in which the performance of one objective function cannot be improved without worsening at least one other objective function [8,50].

3.1. ε-constraint method

3.1.1. Classic formulation

One of the most common and efficient techniques for solving multi-objective problems with MILP optimization is the ε-constraint method [8], where the multi-objective problem is transformed into several single-objective optimization problems, as shown in (47), by using an iterative approach. In particular, only the first objective function is optimized, while the others are constrained to be higher than a constant value e_k^{it}, which is modified in every iteration it. By varying e_k^{it} between the maximum ($\bar{e}_k$) and minimum ($\underline{e}_k$) values of each objective function, calculated beforehand, the procedure is able to calculate the Pareto frontier [8,50]. It is worth noticing that the maximum and minimum values of e_k^{it} are calculated by solving p optimization problems corresponding to the maximization of each $f_k(\mathbf{x})$ one at a time, disregarding the other $f_{j\neq k}(\mathbf{x})$. The results are stored in the payoff table and upper and lower bounds for each objective function are identified.

$$\begin{aligned}
&\max f_1(\mathbf{x})\\
&s.t. f_2(\mathbf{x}) \geq e_2^{it}\\
&\quad f_3(\mathbf{x}) \geq e_3^{it}\\
&\quad \dots\\
&\quad f_p(\mathbf{x}) \geq e_p^{it}\\
&\quad y_i(\mathbf{x}) \leq 0 \qquad i \in 1...m\\
&\quad h_l(\mathbf{x}) = 0 \qquad l \in 1...q\\
&\quad \mathbf{x} = [x_1, x_2, \dots, x_n]^T
\end{aligned} \tag{47}$$

As typically done, the parameters e_k^{it} span between $\bar{e}_k$ and $\underline{e}_k$ with a uniform distribution divided into g_k intervals and $(g_k + 1)$ points, with a resolution of $step_k = \frac{r_k}{g_k}$, where $r_k = \bar{e}_k - \underline{e}_k$ represents the range of variation of the objective function k. With this formulation, each optimization (47) is carried out on a specific subspace of the search space, which can be described as a p-dimensional matrix of points. For every iteration it, the values of parameters e_k^{it} can be calculated as $e_k = \underline{e}_k + i_k^{it} \cdot step_k$, where $i_k^{it} \in \{1, \dots, g_k + 1\}$ is the integer value representing the current position in the grid.

The total number of points in the grid is $(g_2 + 1) \cdot (g_3 + 1) \cdot \dots \cdot (g_k + 1)$, which leads to an exponential behaviour. Therefore, the computational complexity can be very challenging as the number of objective functions increases.

When the optimization of a grid point leads to a better performance with respect to the thresholds forced by the vector $\mathbf{e}$, all the optimizations with intermediate positions of $\mathbf{e}$ will be characterized by very similar results (exactly the same Pareto point in case of null optimality gap). Moreover, the information from initial optimizations used to identify the limits of the e_k^{it} parameters is not used in the main iterative algorithm (47). This means that the standard ε-constraint method can lead to a large number of redundant optimizations that significantly increases the computational requirements.

3.1.2. AUGMECON2

The augmented ε-constraint method, a significant improvement of the ε-constraint method, was proposed by Mavrotas and named AUGMECON2 in its most recent development [38,39]. Conversely to the classic approach in which the extreme values ($\bar{e}_k$ and $\underline{e}_k$) of the objective functions are calculated by simply optimizing one objective function at a time, AUGMECON2 makes use of lexicographic optimization for every objective function: problem (48), with J initially empty, is sequentially solved over the set of p objective functions by adding at the end of every iteration the constraint ($f_j(\mathbf{x}) \geq \hat{f}_j$) updating J. This guarantees that the forthcoming optimization does not deteriorate the optimality of the previous objective functions, as $\hat{f}_j$ represents the best value of objective function j. This limits the search space only to Pareto optimal solutions. The procedure is solved p times, covering the entire set of objective functions, for a total of p^2 optimization problems to solve.

$$\begin{aligned}
&\hat{f}_k = \max\ f_k(\mathbf{x})\\
&s.t. f_j(\mathbf{x}) \geq \hat{f}_j \qquad j \in J\\
&\quad y_i(\mathbf{x}) \leq 0 \qquad i \in 1...m\\
&\quad h_l(\mathbf{x}) = 0 \qquad l \in 1...q\\
&\quad \mathbf{x} = [x_1, x_2, \dots, x_n]^T
\end{aligned} \tag{48}$$

Moreover, problem (47) is modified as follows, where $\mathbf{s} = [s_2, s_3, \dots, s_p]^T$ is the vector of slack variables introducing a penalty when objective functions do not correspond to their desired values e_k^{it}, eps is an adequately small number:

$$\begin{aligned}
&\max(f_1(\mathbf{x}) + eps \cdot (s_2/r_2 + 10^{-1} \cdot s_3/r_3 +\\
&\quad + \dots + 10^{-(p-2)} \cdot s_p/r_p))\\
&s.t. f_2(\mathbf{x}) - s_2 = e_2^{it}\\
&\quad f_3(\mathbf{x}) - s_3 = e_3^{it}\\
&\quad \dots\\
&\quad f_p(\mathbf{x}) - s_p = e_p^{it}\\
&\quad y_i(\mathbf{x}) \leq 0 \quad i \in 1...m\\
&\quad h_l(\mathbf{x}) = 0 \quad l \in 1...q\\
&\quad \mathbf{x} = [x_1, x_2, \dots, x_n]^T
\end{aligned} \tag{49}$$

This configuration of the objective function allows avoiding weakly efficient points. Moreover, to partially reduce the above stated problem of the presence of redundant points, the ratio $s_2/step_2$ is exploited to bypass the redundant points of the innermost loop only, i.e. the loop on e_2. This is a significant limitation that would lead to a considerable increase in computational requirements when more than two objective functions are used.

3.2. The novel A-AUGMECON2

Even if AUGMECON2 is one of the most efficient multi-objective methodologies, the computational burden is still a big issue, especially for computationally intensive algorithms like the one detailed in Section 2; hence inefficiencies, such as redundant simulations, shall be preemptively removed.

The number of grid points to be analysed grows exponentially with the number of objective functions and with the desired density of the Pareto curve. Moreover, the curve tends to present conglomerates of almost identical points, not of interest for the decision maker. This is due to the fact that the very valuable information contained in the slack variables is only used by AUGMECON2 to bypass redundant points on the innermost loop.

A-AUGMECON2, whose source code is publicly available (see Appendix), tackles the problem by limiting the calculation of points only to those whose embedded information is worth to be included in the curve, thus minimizing the computational time.

Two main actions allow limiting the number of points computed:

1. Redundant simulations are preemptively recognized and not performed for all objective functions: slack variables $\mathbf{s}$ are used to identify the redundant grid points.
2. Redundant simulations corresponding to the points obtained to draw the extreme points ($\bar{e}_k$ and $\underline{e}_k$) of the search space are not repeated.

3.2.1. Computation of the payoff table

The priority order adopted in AUGMECON2 for the lexicographic optimization of the payoff table, does not reflect the optimization order used in the iterative algorithm for the creation of the Pareto frontier; hence, payoff table points cannot be used to remove simulations in the following step. Conversely, the priority among the objective functions

Table 2
Priority order in lexicographic optimization for $p = 3$, in AUGMECON2 and A-AUGMECON2.

	AUGMECON2			A-AUGMECON2		
$it = 1$	$f_1 \rightarrow$	$f_2 \rightarrow$	f_3	$f_1 \rightarrow$	$f_2 \rightarrow$	f_3
$it = 2$	$f_2 \rightarrow$	$f_3 \rightarrow$	f_1	$f_2 \rightarrow$	$f_1 \rightarrow$	f_3
$it = 3$	$f_3 \rightarrow$	$f_1 \rightarrow$	f_2	$f_3 \rightarrow$	$f_1 \rightarrow$	f_2

is designed in A-AUGMECON2 to reflect the procedure of the iterative loop and avoid redundant optimizations.

To achieve this, the priority order of the objective functions in the lexicographic optimization needs to be modified in such a way that, instead of simply following the order in which the objective functions are listed in the set as in AUGMECON2, once the kth objective function with the highest priority has been optimized, the second highest priority is attributed to $f_1(\mathbf{x})$; after these two rounds, the rest of the objective functions can be sequentially optimized following the order in which they are listed in the set. As in AUGMECON2, constraints are added at the end of every iteration to prevent the optimizer from worsening the optimality of the previous solutions. The mathematical description is detailed in Algorithm 1.

Algorithm 1 Defining the bounds with the new priority order for lexicographic optimization.

1: **for** $k \in \{1, 2, ..., p\}$ **do**
2: **for** $kk \in \{1, 2, ..., p\}$ **do**
3: **if** $kk = 1$ **then**
4: Solve (48) with $f_{j=k}(\mathbf{x})$ obj. function; store solution $\hat{f}_{k,k}$
5: **else if** $kk \leq k$ **then**
6: Solve (48) with $f_{j=kk-1}(\mathbf{x})$ obj. function; store solution $\hat{f}_{k,kk-1}$
7: **else**
8: Solve (48) with $f_{j=kk}$ obj. function; store solution $\hat{f}_{k,kk}$
9: Add constraint $f_j(\mathbf{x}) \geq \hat{f}_j$
10: Save final solution into payoff table
11: Calculate bounds: $\underline{e}_k = \min_{\hat{k} \in \{1..p\}} \hat{f}_{\hat{k},k}$ and $\bar{e}_k = \max_{\hat{k} \in \{1..p\}} \hat{f}_{\hat{k},k}$

For the sake of clarity, Table 2 compares the order followed in the lexicographic optimization for the computation of the payoff table in AUGMECON2 and A-AUGMECON2, in the case of p=3 objective functions. While the former simply follows the order in which the objective functions are listed in the pertaining set, the latter employs Algorithm 1 to always have f_1 as second highest priority (besides the first optimization, in which it is optimized as first). The A-AUGMECON2 approach allows to obtain a payoff table that contains points belonging to the Pareto curve; those points can be automatically included in the final results, thus avoiding their re-optimization in the iterative procedure to build the Pareto frontier.

Moreover, the hard constraints on the objective functions introduced by the sequential optimizations (see line 9 of Algorithm 1) are turned into soft constraints, i.e. penalties are associated to the differences from the desired values $\hat{f}_j$, in order to avoid infeasibilities that may occur in case of non-null optimality gap.

3.2.2. Construction of Pareto frontier with online filter

The procedure to find the efficient solutions is shown in Fig. 3 and described in this section.

First, the payoff table is completed and the ranges of variation r_k of objective functions $f_2(\mathbf{x}), \ldots, f_p(\mathbf{x})$ are divided into g_k intervals to identify the grid of $(g_2 + 1) \cdot (g_3 + 1) \cdot \ldots \cdot (g_k + 1)$ points, corresponding to the maximum number of iterations to be performed, as detailed in the previous section. Then, after the initialization of given indexes, the main iterative loop starts.

In order to improve the computational performances and the readability of the results, an online filter skipping the redundant points is implemented in every iteration. Each point is associated with a parameter $v_{i_2,\ldots,i_p}$, where $\mathbf{i} = [i_2, \ldots, i_p]^T$ is the position vector of the point in the grid. The parameter has value 1 if the point shall be analysed, 0 if it shall be skipped. At the beginning of the procedure, the vector $\mathbf{v}$ of all $v_{i_2,\ldots,i_p}$ is initialized to analyse all points (vector of ones).

The optimization of a given iteration is performed only if the corresponding $v_{i_2,\ldots,i_p}$ equals 1 and if the position of the point in the grid does not correspond to a point already calculated in the payoff table. If this last condition occurs, the results obtained from the lexicographic optimization to form the payoff table, as per Section 3.2.1, are directly included in the Pareto frontier, thus avoiding the repetition of its calculation.

When the current iteration corresponds to a non-redundant solution, then the optimization is performed and the outcome is collected; when a non-feasible solution is returned, points characterized by more stringent thresholds are skipped, as they are expected to provide non-feasible solutions, too.

When a feasible solution is obtained, it is stored in the repository of the Pareto curve and the result is analysed to evaluate whether some redundant simulations shall be removed by setting the corresponding $v_{\mathbf{i}} = 0$. To do so, the bypass coefficient $b_k = floor(s_k/step_k) + 1$ is computed for $k = 2, \ldots, p$, where $floor(\cdot)$ returns the integer part of the number. Then, Algorithm 2 is adopted to determine all the N_{comb} combinations of $i_2, \ldots, i_p$ identifying the points of the grid that would produce a similar result, where $comb$ and Δi_k are parameters and $mod(\cdot)$ is a function that returns the remainder of the division. The parameter $v_{i_2,\ldots,i_p}$ of the N_{comb} redundant points is set to zero.

Algorithm 2 Defining the positions of redundant points.

$b_k = floor(s_k/step_k) + 1,\ k \in 1, 2, ..., p$
$N_{comb} = \prod_{k=2}^{p} b_k$
for $comb \in 0, ..., N_{comb} - 1$ **do**
  for $k \in 2, ..., p$ **do**
    $\Delta i_k = mod(comb/b_k)$
    $comb = floor(comb/b_k)$
    $i_k = i_k + \Delta i_k$
  $v_{i_2,\ldots,i_p} = 0$

Finally, the parameters $i_2, \ldots, i_p$ are updated to move forward in the grid. The procedure stops when the condition $i_k = g_k + 1$ holds for $k = 2, \ldots, p$.

For the sake of clarity, Fig. 4 illustrates the procedure in presence of redundant optimizations for the case of p=3 objective functions, where $f_1(\mathbf{x})$ is optimized, while $f_2(\mathbf{x})$ and $f_3(\mathbf{x})$, both varying in the range 1÷4, are turned into constraints. Point U_{it}, identified by the green square, is the grid element to be analysed. It lies in position $\mathbf{i}_U = [2, 1]$, i.e. problem (49) is subject to the constraints $(f_2(\mathbf{x}) - s_2 = 2)$ and $(f_3(\mathbf{x}) - s_3 = 1)$. As $v_{\mathbf{i}_U} = 1$, the optimization is not redundant and must be carried out. The problem corresponding to the grid point U_{it} is solved; the results, shown in Fig. 4, are characterized by $s_2 = 1$ and $s_3 = 2$. Applying Algorithm 2, $v_{\mathbf{i}}$ is set to zero for $N_{comb} = 6$ points, including the current grid point and 5 redundant iterations, represented as red dots in Fig. 4. Then, the grid is crossed in the direction of the blue arrow, according to the order in which objective functions are listed in the related set, i.e. along f_2 first, then along f_3. Therefore, the following point to be analysed is U_{it+1}.

4. Case study

4.1. Description

The proposed methodology has been tested on the case study of the rural community of Soroti, Uganda, accounting for about 100

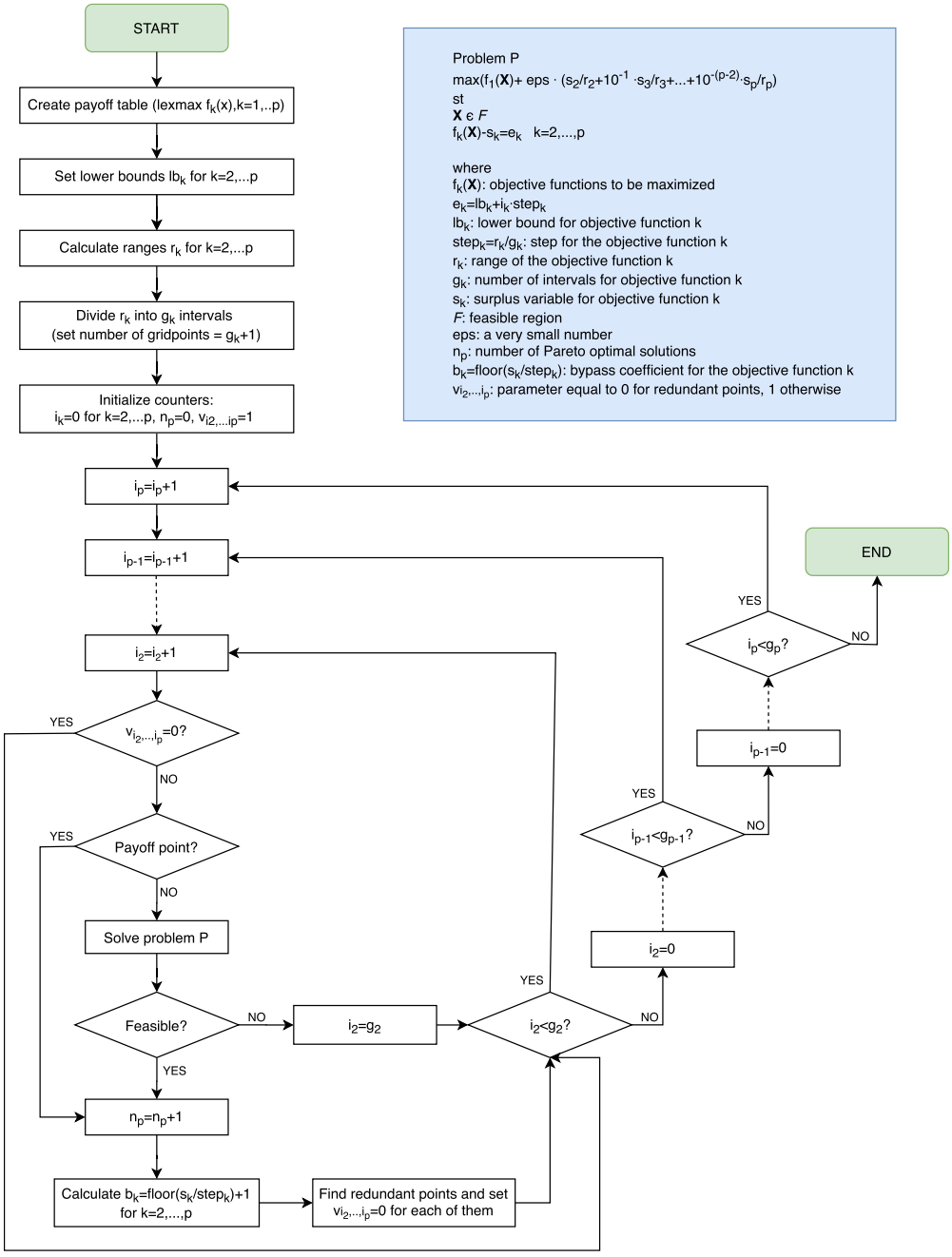

Fig. 3. Flowchart of the proposed methodology.

households and small commercial activities. Given the location and climate of the site, a photovoltaic plant and a wind farm are possible technology candidates for the system along with lithium storage and fuel-fired generation, as shown in Fig. 1.

4.2. Load and renewable production

The initial load curve, shown in Fig. 5, has been estimated in [51] by means of on-field surveys and stochastic analysis, which have observed limited seasonal variations due to the proximity of the area to the Equator. A 2% annual growth has been considered [52].

The specific renewable and wind power production per unit of asset has been estimated using the Renewable.ninja platform [53,54].

4.3. Input parameters

According to the proposed multi-objective approach aligned with the Sustainable Development Goals, the three sustainability dimensions, economic, environmental and social, have been taken into account. The main economic parameters of the optimization are summarized in Table 3; the data related to the environmental impact (global CO2 emissions and land use) are reported in Table 4; the information related to job creation is shown in Table 5, and the need for public lighting has been estimated based on on-field data collection [51].

It is worth noticing that, in order to investigate the global environmental impact of the proposed systems, the emissions have been evaluated with an LCA approach that allows a more in-depth and accurate impact analysis with respect to an evaluation limited to direct emissions alone. The assessment of the local environmental impact of the electrification project has been accounted for in terms of land use

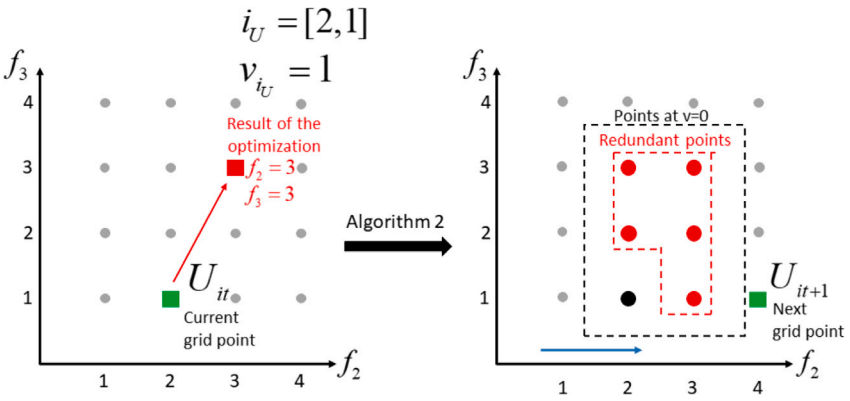

Fig. 4. Procedure to skip redundant optimizations in case p=3.

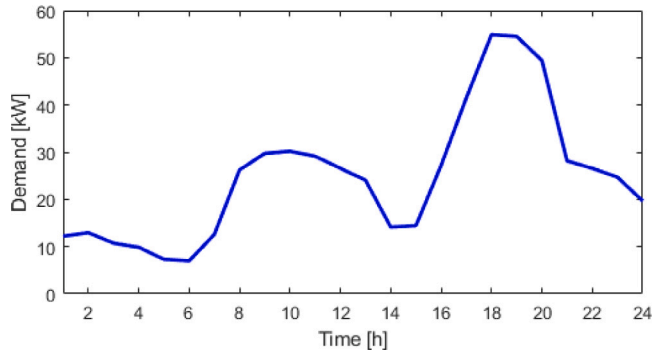

Fig. 5. Initial daily load.

Table 3
Components costs and lifetimes [11,14,17,55].

	Unit size	c_i	m_i	FC_i	Lifetime
Photovoltaic panel	1 kW	1.1 k€	10 €/y	–	20 y
Wind turbine	10 kW	27 k€	810 €/y	–	20 y
Diesel generator	16 kW	11 k€	0.208 €/h	0.75 €/L	15,000 h
Battery	1 kWh	0.4 k€	10 €/y	–	15 y
Converter	1 kW	0.3 k€	–	–	20 y

Table 4
Components LCA emissions and land use [30,56,57].

	Emissions	Land use
Photovoltaic panel	2472.07 $kgCO_2$/kW	7.1 m^2/kW
Wind turbine	935.57 $kgCO_2$/kW	267.7 m^2/kW
Diesel generator	192.17 $kgCO_2$/kW	2.35 m^2/unit
Fuel	3.15 $kgCO_2$/L	–
Battery	56.45 $kgCO_2$/kWh	–

of the different components. As for batteries, their space requirements are considered negligible, as racks can present a very compact layout.

Many studies have analysed the impact of different energy technologies on the job market in industrialized countries [58,59], but little has been done to investigate this topic for rural communities in the Global South. A methodology has been developed in order to estimate multiplicative factors that allow the data of industrialized countries to be applied to different contexts [60]. Given the interest of this work in evaluating the local impacts in terms of job creation, only construction and installation (C&I) and operation and maintenance (O&M) are included and shown in Table 5, as the manufacturing of components for rural electrification projects is very likely to be performed abroad, not contributing to local development.

Asset degradation has been included in the analysis by considering a 1% annual decay of PV panel [18], a 0.53% annual deterioration of wind turbines [19], and a non-linear power-dependent degradation of batteries [62–64].

Table 5
Components job creation per phase [61].

	C&I [jobs/MW]	O&M [jobs/MW]	Fuel [jobs/GWh]
Photovoltaic panel	13.46	7.34	–
Wind turbine	3.06	4.90	–
Diesel generator	2.08	1.96	2.94

Table 6
Computational performances with and without online Pareto pruning.

	Points	Computation time
AUGMECON2	240	95 h
A-AUGMECON2	139	49 h

4.4. Test procedure

The multi-objective problem described in Section 2 has been modelled in GAMS 24.0.2 and solved with CPLEX, using A-AUGMECON2 method described in Section 3.2. The comparison with the standard AUGMECON2 algorithm is also proposed.

The simulations have been run on a 6-core 3.20 GHz Intel Core i7 computer with 16GB RAM. A tolerance of 0.5% has been set on thresholds **e**, $g_k = 6$ for $k \in \{2, \dots, p\}$; hence, a grid of $\prod_{k=2}^{p}(g_k + 1) = 2401$ points is analysed. Each optimization is bound by a time limit of 30 min and the time frame under study is 10 years, described by means of one representative day per month.

5. Results

5.1. Validation of the online Pareto pruning

Table 6 confirms that the novel methodology described in Section 3.2 allows a considerable reduction of the computational burden by skipping many redundant computations, while keeping the same quality of information about the Pareto curve. In particular, the total number of points in the curve is reduced by 42% with respect to the AUGMECON2 method, and the total time employed by A-AUGMECON2 is 48% lower. Hence, the tractability of the problem is highly improved.

In terms of Pareto frontier, Fig. 6 highlights the quality of the results as the two curves show negligible differences, even though A-AUGMECON2 presents 42% fewer points. This means that the adoption of the proposed approach leads to better computational performances, tractability of the results and effectiveness of visualization, thus favouring a more efficient decision making process.

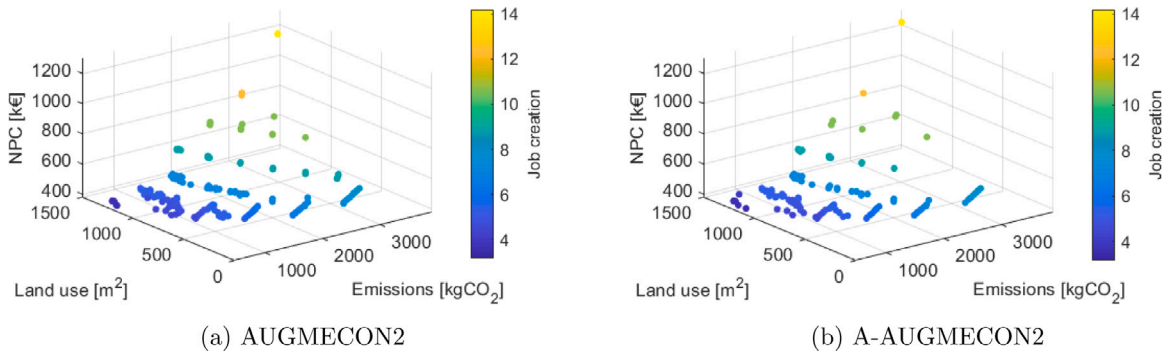

Fig. 6. Comparison of the Pareto curves.

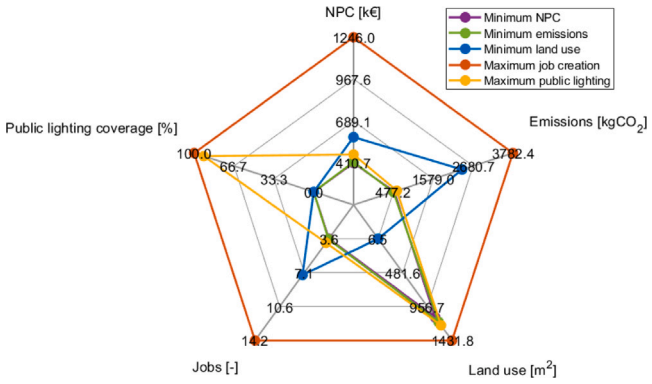

Fig. 7. Payoff table points.

Table 7
Sizing of payoff table points.

	DG* [kW]	PV [kW]	WT [kW]	BESS [kWh]
min NPC	16 (1)	156	0	462
min $CO2$	16 (1)	165	0	481
min LU	32 (2)	0	0	121
max JC	80 (5)	200	0	236
max PL	16 (2)	171	0	513

*: in brackets the number of installed units.

5.2. Discussion on numerical results

The algorithm deals with conflicting objectives and the search space is delimited by the points identified in the payoff table, in which the best performance of each objective function is evaluated as per Section 3.2.1. Fig. 7 shows the value of the different objective functions in the payoff table points, highlighting the main trade-offs between these quantities, while Table 7 presents the units installed for each of these points.

The most significant takeaway is practical overlap of the points at minimum NPC (purple) and minimum emissions (green). This suggests that the economic objective automatically meets the environmental targets, given the technology and cost improvements of the recent years. The curve at maximum public lighting service (yellow), besides satisfying completely the security target, presents negligible differences with the two aforementioned solutions in terms of all the other objective functions, which means that it is also an affordable service and thus it may be recommended for new microgrid installations. However, these three solutions have a significant impact in terms of land use (about 1000m^2). On the other hand, the minimization of land use (blue) manages to reduce the space requirement down to 6m^2 by heavily relying on diesel production, thus significantly increasing both NPC and emissions, although higher local jobs are created due to local maintenance and fuel procurement of the generators. Finally, the curve related to job creation (red) refers to the maximum employment of local human capital, associated to a surge in economic and environmental costs. These results highlight the similarities and differences between the extremes of the solutions to be investigated by local developers and governments, underlining the need for properly developing multi-objective methodologies that assist policy and business decision making.

Table 7 details the optimal design corresponding to the solutions of the payoff table, whose objectives are shown in Fig. 7. It is worth noticing that the solutions focusing on the minimization of NPC and CO2 emissions are very similar also in terms of optimal sizing; the use of PV systems and batteries in the CO2 case is only 4%–6% higher than in the NPC case. Moreover, the only solution where no PV devices are installed corresponds to the minimization of land use, and this result justifies the sharp increase in CO2 emissions with respect to the least-cost option shown in Fig. 7. This shall further guide policy makers and developers in fostering renewable sources and support public lighting, in areas where a relatively large land use is acceptable; yet, the Pareto frontier will be needed to identify the specific trade-off.

The renewable penetration of the solutions of the payoff table spans between 0% (e.g. LU case) till about 98% in the least CO2 emission case. Interestingly, the LCA approach for emissions accounting leads to a generating portfolio of the point at minimum emissions that is not entirely based on renewable sources: the diesel generator is occasionally employed at the end of the project, when the load is higher and the performances of PV panels are poorer. This is because the installation of an additional quantity of panels sufficient to cover the load for the entire duration of the project, net of the degradation phenomena, would cause a greater quantity of life-cycle emissions than those associated with the installation and occasional use of a diesel generator, providing about 2% of the total energy. This result highlights the importance of an LCA impact assessment (from cradle to grave), because limiting the analysis to direct emissions could lead to distorted and incorrect considerations, driving sub-optimal business and policy outcomes.

Furthermore, Fig. 8 compares the different use of resources in the configurations of the payoff table, in order to highlight the energy shares and the impact of multi-year characteristics, namely demand growth and asset degradation. The point at maximum jobs is not included in the analysis, as it corresponds to the installation of all the available units and the employment of the technologies that contribute the most to jobs creation in O&M phase, namely fuel-fired generators; hence, the full demand (including public lighting) is easily fulfilled by DG units. On the other side, the yearly cap on the energy-not-served (ENS) is always hit in all the other points (see Fig. 8), as it enables a reduction of costs, emissions and land use.

In the least-cost solution in Fig. 8(a), the demand of households and productive activities is entirely met by PV panels up to year 5. Then, as the load increases and the equipment degrades, the need to dispatch

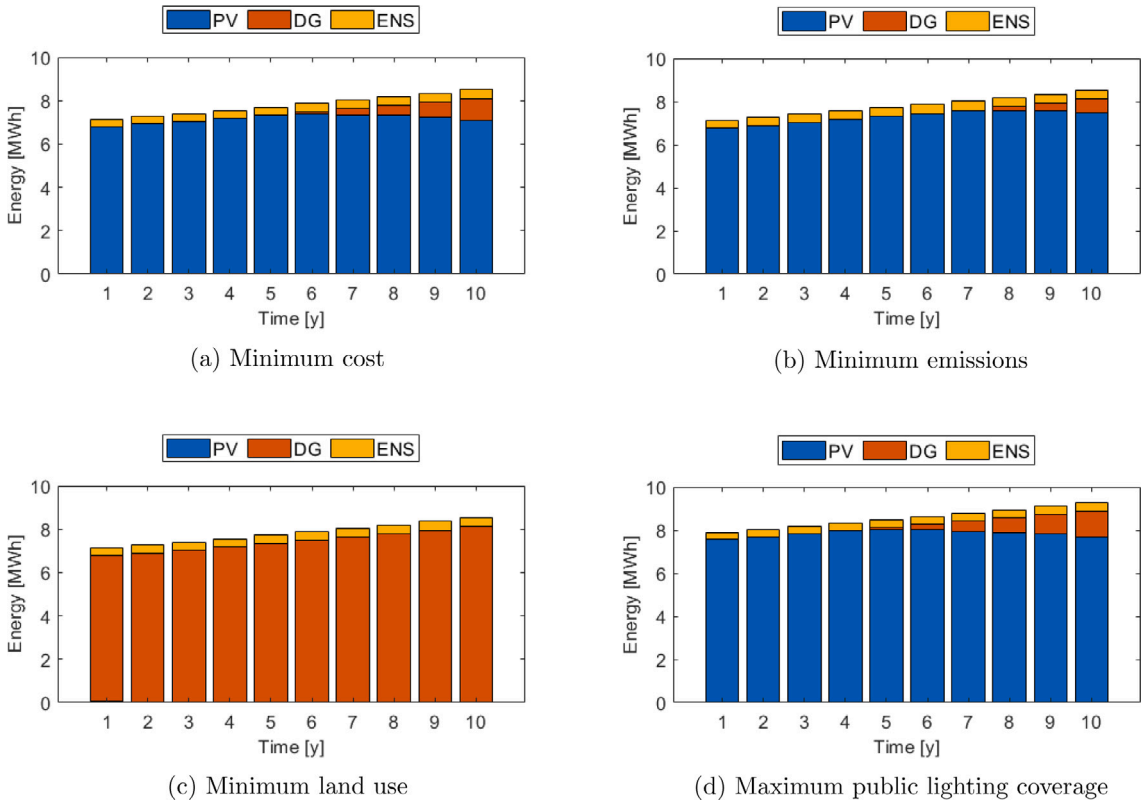

Fig. 8. Yearly dispatching of resources.

DG units gradually increases, up to about 12% of the total demand in year 10. The trends related to the solutions minimizing CO2 emissions (Fig. 8(b)) and maximizing the public lighting (Fig. 8(d)) show very similar behaviour to the least-cost solution(Fig. 8(a)), confirming that reduction of emissions is compatible with cost-effective designs and that public lighting can be met without significantly increasing the generation costs. In particular, the contribution of fuel-fired generators in the last year accounts for about 8% in the minimum CO2 and 13% in the maximum public lighting solution respectively. On the contrary, when land use is minimized (Fig. 8(c)), the demand is fully met by the fuel-fired generators or curtailed; no renewable sources are employed.

5.3. Narrowing down possible solutions

Despite the filter, which removes redundancies and improves the readability of the results, some considerations can be made to further reduce the portfolio of available options and ease the decision making process, starting from the analysis of Figs. 7 and 6(b) and from the considerations in Section 5.2. In particular, the points of the grid with high thresholds on jobs creation (> 8) can be excluded from the analysis, as they correspond to oversized microgrids. Moreover, given the limited influence of public lighting on the total cost of the system, it is sensible to guarantee a high share of the service, in light of the extremely positive impact it has on the well-being of the community. Therefore, only points with $PL > 90\%$ are taken into consideration. This allows to narrow the options down to the 15 points shown in Fig. 9. Such reduced selection of points supports the decision maker in a more straightforward visualization of the trade-off between the objective functions, while preserving a rich portfolio of solutions.

Fig. 9(a) highlights that higher emissions are associated with higher costs and more people employed in the plant. The top-right area of the graph corresponds to the points with the lowest renewable fraction: the higher the reliance on diesel generators, the greater the emissions and the workforce needed to manage maintenance and fuel procurement. Moreover, these points are also characterized by very limited land use, as shown in Fig. 9(b), as diesel generators cover very limited space, unlike PV panels. It is worth noticing that comparable levels of land use, which, as a matter of fact, means similar PV capacity, correspond to wide ranges of emissions and costs, as the effectiveness in exploiting solar energy is strongly related to the capacity of the storage system. This, in turn, determines the need for diesel generators, whose operation significantly affects NPC and emissions.

A closer look on the selected points is provided in Fig. 10, where the technical design and costs breakdown of the points in Fig. 9 are shown in relation to LCA emissions. In particular, Fig. 10(a) further underlines the impact of storage on the effective exploitation of renewable resources: BESS capacity is needed along with the renewable assets (PV panels) to further decrease CO2 emissions. On the other hand, the higher the reliance on fuel-fired generators, the lower the CAPEX, thus the implementing entity can defer costs, reducing the initial investment at the cost of higher expenses along the project lifetime and larger CO2 emissions (see Fig. 10(b)). This element could have a decisive weight during the decision process, depending on the availability of funds, local regulation and company goals.

5.4. Decision making process

The peculiarity of the Pareto curve obtained from multi-objective optimization is that it preserves the complexity of the problem under analysis and allows the decision maker to have a full picture of the possible solutions and of their outcomes in different scopes.

Several works adopt procedures that lead to the selection of one single point of the curve by means of mathematical methods [45,46]. In the authors' opinion, the selection of the optimal microgrid for the purpose of rural electrification has so many impacts on the community, that it is preferable that the decision maker is able to evaluate among a reasonable number of options and to select the most appropriate according to site-specific characteristics.

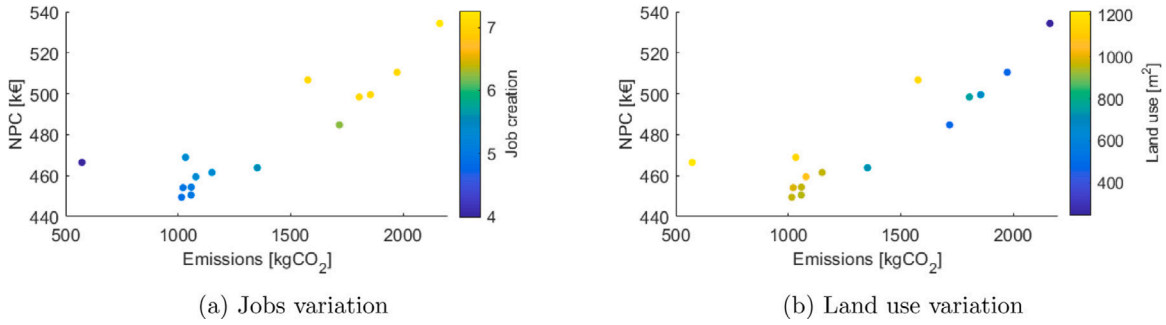

Fig. 9. Reduced Pareto curve.

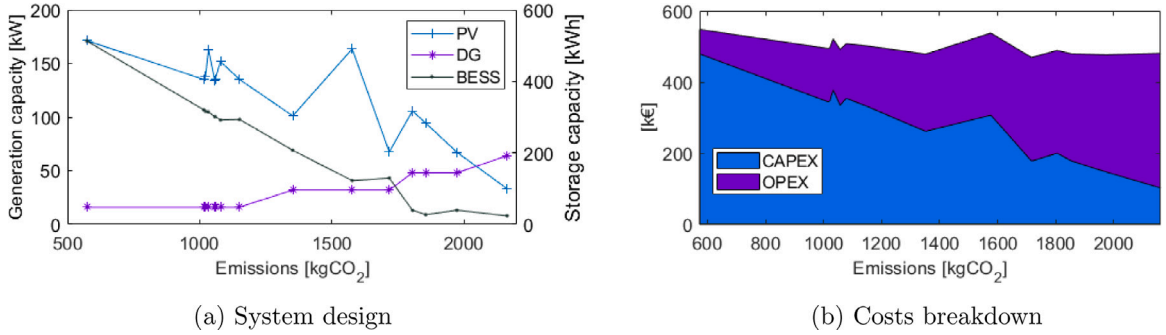

Fig. 10. Technical and economical performances of the selected Pareto points.

Among the various qualitative criteria that can facilitate the final evaluation based on the specificities of the community are: the willingness to pay for energy; the social acceptability of the different technologies; the compatibility with future expansion of the plant; the resilience of the system, related to the availability of components and to the ease of maintenance and training of specialized personnel [29,30,32].

6. Conclusions

This paper successfully proposes a multi-objective planning method for off-grid microgrids able to optimize socio-economic, security and environmental concerns in a long-term perspective, accounting for detailed multi-year simulations of the system operation and assets degradation. In order to efficiently solve the corresponding non-linear multi-objective problem, the novel A-AUGMECON2 algorithm has been developed and its results proved to improve the convergence characteristics of the standard AUGMECON2, thanks to the novel Pareto pruning method that avoids repeating redundant optimizations. Each A-AUGMECON2 optimization is integrated with an iterative approach that allows to efficiently deal with the non-linear problem by solving a number of MILP subproblems, where parameters are updated till convergence.

The results, obtained on a case study of a typical microgrid in Uganda, highlight that the least-cost solution tends to be aligned to the minimization of life cycle emissions, with less than 1%–5% difference in each objective function; hence, economic and environmental targets can be met conjointly. Moreover, meeting the security goal, expressed by the public lighting penetration, increases costs by less than 10%, with considerable social benefits, thus recommending to decision makers to include this service when planning rural electrification projects. On the other hand, maximizing local jobs and minimizing land use bring about a surge in costs, implying that when these needs are relevant, policy and business decision makers shall carefully select the optimal design and find the best compromise on the Pareto frontier, according to the specific needs of the community. These results, efficiently obtained by the proposed methodology, highlight the need for multi-objective multi-year optimization tools for optimizing rural microgrids in the Global South.

Moreover, the proposed methodology based on the novel A-AUGMECON2 has confirmed to reach the same optimal Pareto frontier than standard approaches (AUGMECON2) but with roughly half the computational requirements of the latter. This proves the approach discussed in this paper to be an adequate tool to foster the practical use of multi-objective multi-year methodologies by developers and policy makers, given their constant need for fast optimization tools with far-reaching long-term perspective.

Future developments of the work may include the evaluation of the stochasticity of long-term scenarios and the integration of multiple investment steps along the project lifetime. Furthermore, the proposed methodology can be applied to a large variety of energy systems, thus benefiting both policy/business decision makers and the research community, who may infer more accurate results and better tailor their projects, thus enabling cost savings, environmental benefits and improved social well-being.

Appendix. Source code

The source code is publicly available on the GitHub platform at the following link: https://github.com/marinapet/multi-objective.

References

[1] UN Economic and Social Council. Progress towards the sustainable development goals. Report of the secretary-general, 2020, p. 1–23.
[2] Riva F, Ahlborg H, Hartvigsson E, Pachauri S, Colombo E. Electricity access and rural development: Review of complex socio-economic dynamics and causal diagrams for more appropriate energy modelling. Energy Sustain Dev 2018;43:203–23.
[3] Kurdziel M-J, Thomas D. The role of renewable energy mini-grids in Kenya's electricity sector evidence of a cost-competitive option for rural electrification and sustainable development. In: Ambition to ation. Tech. rep., 2019, November.
[4] Riva F, Tognollo A, Gardumi F, Colombo E. Long-term energy planning and demand forecast in remote areas of developing countries: Classification of case studies and insights from a modelling perspective. Energy Strategy Rev 2018;20:71–89.

[5] IEA. World energy outlook 2020. Tech. rep., 2020.
[6] Cuesta MA, Castillo-Calzadilla T, Borges CE. A critical analysis on hybrid renewable energy modeling tools: An emerging opportunity to include social indicators to optimise systems in small communities. Renew Sustain Energy Rev 2020;122:109691.
[7] Berizzi A, Bovo C, Innorta M, Marannino P. Multiobjective optimization techniques applied to modern power systems. In: 2001 IEEE power engineering society winter meeting. 2002, p. 1503–8.
[8] Chiandussi G, Codegone M, Ferrero S, Varesio FE. Comparison of multi-objective optimization methodologies for engineering applications. Comput Math Appl 2012;63(5):912–42.
[9] Moshi GG, Bovo C, Berizzi A, Taccari L. Optimization of integrated design and operation of microgrids under uncertainty. In: 19th power systems computation conference. 2016.
[10] Li B, Roche R, Miraoui A. Microgrid sizing with combined evolutionary algorithm and MILP unit commitment. Appl Energy 2017;188:547–62.
[11] Moretti L, Astolfi M, Vergara C, Macchi E, Pérez-Arriaga JI, Manzolini G. A design and dispatch optimization algorithm based on mixed integer linear programming for rural electrification. Appl Energy 2019;233–234:1104–21.
[12] Riva F, Gardumi F, Tognollo A, Colombo E. Soft-linking energy demand and optimisation models for local long-term electricity planning: An application to rural India. Energy 2019;166:32–46.
[13] Brivio C, Moncecchi M, Mandelli S, Merlo M. A novel software package for the robust design of off-grid power systems. J Cleaner Prod 2017;166:668–79.
[14] Prathapaneni DR, Detroja KP. An integrated framework for optimal planning and operation schedule of microgrid under uncertainty. Sustain Energy Grids Netw 2019;19:100232.
[15] Pecenak ZK, Stadler M, Fahy K. Efficient multi-year economic energy planning in microgrids. Appl Energy 2019;255(April 2019):113771.
[16] Rossi A, Stabile M, Puglisi C, Falabretti D, Merlo M. Evaluation of the energy storage systems impact on the Italian ancillary market. Sustain Energy Grids Netw 2019;17:100178.
[17] Petrelli M, Fioriti D, Berizzi A, Poli D. Multi-year planning of a rural microgrid considering storage degradation. IEEE Trans Power Syst 2021;36(2):1459–69.
[18] Azizi A, Logerais PO, Omeiri A, Amiar A, Charki A, Riou O, et al. Impact of the aging of a photovoltaic module on the performance of a grid-connected system. Sol Energy 2018;174(August):445–54.
[19] Hamilton SD, Millstein D, Bolinger M, Wiser R, Jeong S. How does wind project performance change with age in the united states? Joule 2020;4(5):1004–20.
[20] Koltsaklis NE, Giannakakis M, Georgiadis MC. Optimal energy planning and scheduling of microgrids. Chem Eng Res Des 2018;131:318–32.
[21] Zhang J, Li KJ, Wang M, Lee WJ, Gao H. A bi-level program for the planning of an islanded microgrid including CAES. In: IEEE industry application society - 51st annual meeting, conference record. 2015, p. 1–8.
[22] Zhao B, Zhang X, Li P, Wang K, Xue M, Wang C. Optimal sizing, operating strategy and operational experience of a stand-alone microgrid on Dongfushan Island. Appl Energy 2014;113:1656–66.
[23] Mashayekh S, Stadler M, Cardoso G, Heleno M. A mixed integer linear programming approach for optimal DER portfolio, sizing, and placement in multi-energy microgrids. Appl Energy 2017;187:154–68.
[24] Abo-Elyousr FK, Elnozahy A. Bi-objective economic feasibility of hybrid microgrid systems with multiple fuel options for islanded areas in Egypt. Renew Energy 2018;128:37–56.
[25] Kharrich M, Mohammed OH, Alshammari N, Akherraz M. Multi-objective optimization and the effect of the economic factors on the design of the microgrid hybrid system. Sustainable Cities Soc 2021;65(October 2020):102646.
[26] Silva D, Nakata T. Multi-objective assessment of rural electrification in remote areas with poverty considerations. Energy Policy 2009;37(8):3096–108.
[27] Hiremath RB, Kumar B, Balachandra P, Ravindranath NH. Bottom-up approach for decentralised energy planning: Case study of Tumkur district in India. Energy Policy 2010;38(2):862–74.
[28] Dufo-López R, Cristóbal-Monreal IR, Yusta JM. Optimisation of PV-wind-diesel-battery stand-alone systems to minimise cost and maximise human development index and job creation. Renew Energy 2016;94:280–93.
[29] Fuso Nerini F, Howells M, Bazilian M, Gomez MF. Rural electrification options in the Brazilian Amazon. A multi-criteria analysis. Energy Sustain Dev 2014;20(1):36–48.
[30] Mainali B, Silveira S. Using a sustainability index to assess energy technologies for rural electrification. Renew Sustain Energy Rev 2015;41:1351–65.
[31] Kumar A, Singh AR, Deng Y, He X, Kumar P, Bansal RC. Integrated assessment of a sustainable microgrid for a remote village in hilly region. Energy Convers Manage 2019;180:442–72.
[32] Juanpera M, Blechinger P, Ferrer-Martí L, Hoffmann MM, Pastor R. Multicriteria-based methodology for the design of rural electrification systems. A case study in Nigeria. Renew Sustain Energy Rev 2020;133:110243.
[33] Li L, Mu H, Li N, Li M. Economic and environmental optimization for distributed energy resource systems coupled with district energy networks. Energy 2016;109:947–60.
[34] Martínez-Gomez J, Peña-Lamas J, Martín M, Ponce-Ortega JM. A multi-objective optimization approach for the selection of working fluids of geothermal facilities: Economic, environmental and social aspects. J Environ Manag 2017;203:962–72.
[35] Zhang D, Evangelisti S, Lettieri P, Papageorgiou LG. Optimal design of CHP-based microgrids: Multiobjective optimisation and life cycle assessment. Energy 2015;85:181–93.
[36] Cambero C, Sowlati T. Incorporating social benefits in multi-objective optimization of forest-based bioenergy and biofuel supply chains. Appl Energy 2016;178:721–35.
[37] Zhong J, Yu TE, Clark CD, English BC, Larson JA, Cheng CL. Effect of land use change for bioenergy production on feedstock cost and water quality. Appl Energy 2018;210:580–90.
[38] Mavrotas G. Effective implementation of the ϵ-constraint method in multi-objective mathematical programming problems. Appl Math Comput 2009;213(2):455–65.
[39] Mavrotas G, Florios K. An improved version of the augmented s-constraint method (AUGMECON2) for finding the exact pareto set in multi-objective integer programming problems. Appl Math Comput 2013;219(18):9652–69.
[40] Jabbarzadeh A, Fahimnia B, Rastegar S. Green and resilient design of electricity supply chain networks: A multiobjective robust optimization approach. IEEE Trans Eng Manage 2019;66(1):52–72.
[41] Wang M, Yu H, Jing R, Liu H, Chen P, Li C. Combined multi-objective optimization and robustness analysis framework for building integrated energy system under uncertainty. Energy Convers Manage 2020;208(February):112589.
[42] Sudeng S, Wattanapongsakorn N. Post Pareto-optimal pruning algorithm for multiple objective optimization using specific extended angle dominance. Eng Appl Artif Intell 2015;38:221–36.
[43] Yan'Gang L, Zheng Q. A decision support system for satellite layout integrating multi-objective optimization and multi-attribute decision making. J Syst Eng Electron 2019;30(3):535–44.
[44] Brusco MJ. Partitioning methods for pruning the Pareto set with application to multiobjective allocation of a cross-trained workforce. Comput Ind Eng 2017;111:29–38.
[45] Wang Z, Rangaiah GP. Application and analysis of methods for selecting an optimal solution from the Pareto-optimal front obtained by multiobjective optimization. Ind Eng Chem Res 2017;56(2):560–74.
[46] Sanchez-Gomez JM, Vega-Rodríguez MA, Pérez CJ. Comparison of automatic methods for reducing the Pareto front to a single solution applied to multi-document text summarization. Knowl-Based Syst 2019;174:123–36.
[47] Mehrjerdi YZ, Shafiee M. A resilient and sustainable closed-loop supply chain using multiple sourcing and information sharing strategies. J Cleaner Prod 2020;289.
[48] Caglayan N, Satoglu SI. Multi-objective two-stage stochastic programming model for a proposed casualty transportation system in large-scale disasters: A case study. Mathematics 2021;9(4):316.
[49] Nikas A, Fountoulakis A, Forouli A, Doukas H. A robust augmented ϵ-constraint method (AUGMECON-r) for finding exact solutions of multi-objective linear programming problems. In: Operational research, no. 0123456789. Springer Berlin Heidelberg; 2020.
[50] Cui Y, Geng Z, Zhu Q, Han Y. Review: Multi-objective optimization methods and application in energy saving. Energy 2017;125:681–704.
[51] Mandelli S, Brivio C, Colombo E, Merlo M. A sizing methodology based on levelized cost of supplied and lost energy for off-grid rural electrification systems. Renew Energy 2016;89:475–88.
[52] Blechinger DP, Papadis E, Baart M, Telep P, Simonsen F. What size shall it be? A guide to mini-grid sizing and demand forecasting. 2016, The German Climate Technology Initiative.
[53] Pfenninger S, Staffell I. Long-term patterns of European PV output using 30 years of validated hourly reanalysis and satellite data. Energy 2016;114:1251–65.
[54] Staffell I, Pfenninger S. Using bias-corrected reanalysis to simulate current and future wind power output. Energy 2016;114:1224–39.
[55] Kamjoo A, Maheri A, Dizqah AM, Putrus GA. Multi-objective design under uncertainties of hybrid renewable energy system using NSGA-II and chance constrained programming. Int J Electr Power Energy Syst 2016;74:187–94.
[56] Rojas-Zerpa JC, Yusta JM. Application of multicriteria decision methods for electric supply planning in rural and remote areas. Renew Sustain Energy Rev 2015;52:557–71.
[57] Martín-Chivelet N. Photovoltaic potential and land-use estimation methodology. Energy 2016;94:233–42.
[58] Cartelle Barros JJ, Lara Coira M, de la Cruz López MP, del Caño Gochi A. Comparative analysis of direct employment generated by renewable and non-renewable power plants. Energy 2017;139:542–54.
[59] Henriques CO, Coelho DH, Cassidy NL. Employment impact assessment of renewable energy targets for electricity generation by 2020—An IO LCA approach. Sustainable Cities Soc 2016;26(2016):519–30.
[60] Institute for Sustainable Futures. Calculating global energy sector jobs 2015 methodology update. 2015, p. 1–48.
[61] Okunlola A, Evbuomwan O, Zaheer H, Winklmaier J. Assessment of decentralized hybrid mini-grids in sub-saharan africa: Market analysis, least-cost modelling, and job creation analysis. In: Africa-EU renewable energy research and innovation symposium 2018. 2018, p. 21–34.
[62] Luo X, Wang J, Dooner M, Clarke J. Overview of current development in electrical energy storage technologies and the application potential in power system operation. Appl Energy 2015;137:511–36.

[63] Haidl P, Buchroithner A, Schweighofer B, Bader M, Wegleiter H. Lifetime analysis of energy storage systems for sustainable transportation. Sustainability 2019;11(23).

[64] Moncecchi M, Brivio C, Mandelli S, Merlo M. Battery energy storage systems in microgrids: Modeling and design criteria. Energies 2020;13(8):1–18.